

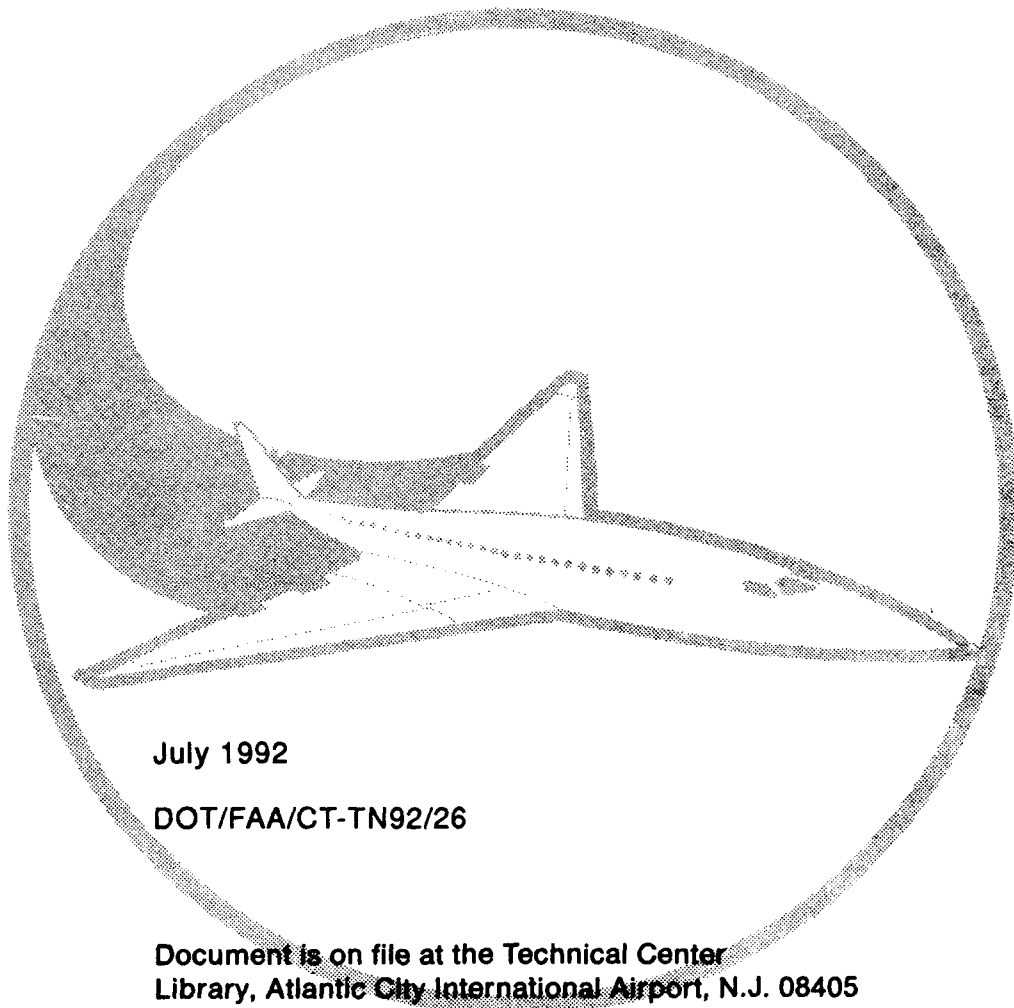
Technical note

AD-A257 639



2

Inspection of Fabricated Fuselage Panels Using Electronic Shearography



July 1992

DOT/FAA/CT-TN92/26

Document is on file at the Technical Center
Library, Atlantic City International Airport, N.J. 08405



U.S. Department of Transportation
Federal Aviation Administration

Technical Center
Atlantic City International Airport, N.J. 08405

8 1992

92-28184



425606

11/10
RVS

NOTICE

This document is disseminated under the sponsorship of the U. S. Department of Transportation in the interest of information exchange. The United States Government assumes no liability for the contents or use thereof.

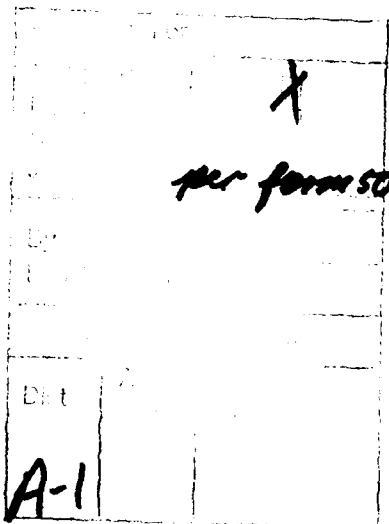
The United States Government does not endorse products or manufacturers. Trade or manufacturers' names appear herein solely because they are considered essential to the objective of this report.

Technical Report Documentation Page

1. Report No. DOT/FAA/CT-TN92/26		2. Government Accession No.		3. Recipient's Catalog No.	
4. Title and Subtitle INSPECTION OF FABRICATED FUSELAGE PANELS USING ELECTRONIC SHEAROGRAPHY				5. Report Date July 1992	
				6. Performing Organization Code	
7. Author(s) John Tyson, II; Ben Feferman				8. Performing Organization Report No.	
9. Performing Organization Name and Address Laser Technology, Incorporated Norristown, PA 19403				10. Work Unit No. (TRAIS)	
				11. Contract or Grant No. DTRS57-90-P-80922	
12. Sponsoring Agency Name and Address U.S. Department of Transportation Federal Aviation Administration Technical Center Atlantic City International Airport, NJ 08405				13. Type of Report and Period Covered Technical Note	
				14. Sponsoring Agency Code ACD-220	
15. Supplementary Notes Volpe National Transportation Systems Center Project Manager: Stephen Bobo FAA Technical Center Project Manager: Dave Galella					
16. Abstract This report describes the results of a proof of principle demonstration of using electronic shearography to detect induced damage in fabricated aircraft panels. The demonstration was performed at the FAA's Aircraft Panel Test Facility in Waltham, Massachusetts and all shearography equipment and its operational support was provided by Laser Technology, Inc. (LTI) under a separate contract from the Volpe National Transportation Systems Center. The test panels that were inspected using the electronic shearography were constructed to closely simulate the fuselage and skin structure of Boeing 727 and 737 aircraft. These panels contained programmed flaws intended to simulate two major types of defects associated with aging aircraft, namely, cracks along fastener rows, and disbonded tear strap doublers and lap joints. The proof of principle consisted of a series of inspections that demonstrated shearography's capability to detect cracks and disbonds in the fuselage panel specimens. The sensitivity of shearography to detect short, simulated fatigue cracks that would correspond to a multiple site damage situation was too low to provide sufficient confidence that the method could economically replace existing eddy current surface methods. The sensitivity of the method to detect panel disbonding, however, is sufficient to encourage further development of the technique.					
17. Key Words Electronic Shearography NDI Lap Joint Disbonding Coherent Light Strain Fields Fuselage Panels Multi Site Damage B-727/B-737			18. Distribution Statement Document is on file at the Technical Center Library, Atlantic City International Airport, New Jersey 08405		
19. Security Classif. (of this report) Unclassified		20. Security Classif. (of this page) Unclassified		21. No. of Pages 41	
				22. Price	

TABLE OF CONTENTS

	Page
EXECUTIVE SUMMARY	vii
INTRODUCTION	1
Purpose	1
Background	1
TEST APPARATUS	2
Test Fixture	2
Test Panels	2
Shearography Instrumentation	3
TEST PROCEDURE	10
TEST SERIES NO. 1 - CONTROL PANEL	12
Results	12
Discussion	13
TEST SERIES NO. 2 - MID-BAY CRACK	18
Results	18
Discussion	19
TEST SERIES NO. 3 - SIMULATED LAP JOINT DISBONDS	27
Results	27
Discussion	28
TEST SERIES NO. 4 - SIMULATED LAP JOINT MSD	32
Results	32
Discussion	32
CONCLUSIONS	35



LIST OF ILLUSTRATIONS

Figure		Page
1	FAA Aircraft Panel Test Facility at Foster-Miller	5
2	Aerial View of Test Fixture Showing Test Panel Laying Horizontally with Edges Held and the ES-9120 on the Frame	5
3	Drawing of Typical Test Panel Showing Locations of Frames, Tear Straps, and Stringers	6
4	Rear View of Test Panel No. 3	7
5	Close Up of Test Panel Construction	7
6	ES-9120 Shearography System Inspecting for MSD Cracking	8
7	Shearography Camera Inspecting Lap Joint	8
8	Illustration of Shearography Theory	9
9	Adjusting Shearography Camera on the Test Fixture	11
10	Shearography Camera's View of the Aircraft Test Panel	11
11	X-vector Shearogram of Aircraft Panel Lap Joint	14
12	Y-vector Shearogram of Aircraft Panel Lap Joint	15
13	Live Image, X-vector Shearogram, and Y-vector Shearogram of the Same Loose Rivet in Test Panel No. 1	16
14	X-vector Shearogram Prior to Where a 10-Inch Mid-Bay Crack Would be Cut into Test Panel No. 1	17
15	Y-vector Shearogram Prior to Where a 10-Inch Mid-Bay Crack Would be Cut into Test Panel No. 1	17
16	Photograph of Test Panel No. 1 with 10-Inch Mid-Bay Crack Shown Horizontally in the Center	20
17	Normal View of the Mid-Bay Crack after Fatigue Cycling to 15 Inches	20
18	High Strain Seen Over Mid-Bay Crack with 0.01 PSI Differential Stressing Pressure in this X-vector Shearogram	21
19	X-vector Shearogram of Mid-Bay Crack at 0.005 PSI Differential Stressing Pressure	22

20	Image of a 45-Degree Vector Shearogram Showing Strain Concentrations Around the Mid-Bay Crack	23
21	Y-vector Shearogram at 0.005 PSI Differential Pressure Showing Strain Concentrations Around the Mid-Bay Crack	24
22	20X Micrograph Showing Crack Tip Area	25
23	200X Micrograph at 0 PSIG Showing the Crack Tip Closed	26
24	200X Micrograph at 5 PSIG with the Crack Tip Open	26
25	First Section of Lap Joint Inspected During Test Series No. 3 Showing Bonded and Disbonded Areas	29
26	Second Section of Lap Joint Inspected During Test Series No. 3 Showing Disbonding and MSD Linkup at the Top of Each Image	30
27	Residual Strain Indicating a Lap Joint Disbond Around a Single Rivet or Possibly an Improperly Loaded Rivet	31
28	Small Fatigue Cracks Around Panel Rivet Hole	33
29	X-vector Shearogram Showing Strain Concentrations Around 0.375-Inch Cracks	33
30	Shearography Camera Sitting On Panel to Closely View MSD Cracking	34
31	Small MSD Cracking Along Upper Line of Rivets	34

EXECUTIVE SUMMARY

For the purpose of investigating emerging methods of nondestructive inspection (NDI), the Federal Aviation Administration (FAA) Technical Center sponsored the Volpe National Transportation System Center (VNTSC) to assess the potential use of electronic shearography for rapid, wide area inspection of aging aircraft structures.

This report describes the results of a proof of principle demonstration conducted on fabricated aircraft panels containing varying degrees of simulated aging aircraft fatigue damage. The demonstration was performed at the FAA's Aircraft Panel Test Facility in Waltham, Massachusetts. All shearography equipment and its operational support were provided by Laser Technology, Inc. (LTI) under a separate subcontract from the VNTSC. Although all system operation was performed by LTI personnel, the demonstration project was supervised throughout by a VNTSC representative.

The test panels that were inspected using the electronic shearography were constructed to simulate the fuselage and skin structure of Boeing 727 and 737 aircraft. These panels contained flaws intended to simulate two major types of defects associated with aging aircraft, namely, cracks along fastener rows, and disbanded tear strap doublers and lap joints.

The proof of principle consisted of a series of inspections to demonstrate shearography's capability to detect cracks and disbonds in the fuselage panel specimens. The sensitivity of shearography to detect short, simulated, fatigue cracks was too low to provide sufficient confidence that the method could economically replace existing eddy current surface methods. The sensitivity of the method to detect panel disbonding, however, is sufficient to encourage further development of the technique.

Specific findings from the demonstration were:

1. Strain fields of approximately 10 x 14 inches on the fabricated fuselage panels were readily observed as a repetitive pattern from which anomalies such as cracks, disbonds, and improperly loaded rivets were readily discernable.
2. Adequate strain fields were observed by shearography at various pressure load levels imposed on the panels. Applied panel loads used during the shearography demonstrations ranged from 1 to 8 psi. Differential pressure levels as low as 0.005 psi were sufficient to produce interpretable strain patterns. Anomalies in strain patterns at the tips of a large mid-bay crack were easily detected.
3. Although the strain fields around small crack tips were detectable, shearography loses its advantage of large area coverage if used for detection of these fields. To resolve these small cracks, the field of view had to be reduced.
4. The difference in strain fields between disbanded riveted lap joints and well bonded riveted lap joints is sufficient to encourage the

development of shearography as a rapid, broad area technique for mapping disbonds in fuselage tear strap doublers and lap joint structures.

5. Like other methods of NDI, proper interpretation of the strain fields produced by the shearography equipment requires adequate training of the inspector. Also, it is critical that the inspector have detailed knowledge of all internal aircraft structure and how that structure will affect the surface strain fields that are imaged by the electronic shearography.

INTRODUCTION

Purpose

Aging aircraft are a concern due to a large number of commercial airliners having exceeded their economic design life, but not having been retired. These aircraft require increased monitoring of their structures and skins for cracks and disbond damage. Current nondestructive inspections (NDI) methods that are used to find these forms of damage are quite tedious and limited in their detection capability.

In order to ascertain the capabilities of prospective inspection techniques, the Department of Transportation's Volpe National Transportation Systems Center (VNTSC) and the Federal Aviation Administration (FAA) Technical Center contracted Laser Technology, Inc. (LTI) to conduct a series of tests to detect various types of age related damage using advanced electronic shearography.

Background

Electronic shearography has been used effectively in testing many types of aircraft materials for defects. Shearography was initially developed as a full field strain gauge. In principle, shearography finds subsurface defects by imaging changes in surface strains induced by these defects. During the shearography inspection, the part under test is stressed and the resultant strain concentrations can reveal the size and location of defects such as cracks and disbonds.

This shearography demonstration program utilized the FAA Aircraft Panel Test Facility which is capable of subjecting full-scale sections of fuselage panels to internal pressurizations. This test fixture simulates the stresses that an aircraft encounters as it climbs to altitude. The cyclic hoop stress due to the pressurization is understood to be the primary mode loading that causes fatigue damage of aircraft fuselages. Shearography's ability to image the resultant local strains across the lap joint and around individual rivets during a slight change of internal pressure was used to locate and characterize simulated fatigue cracking and adhesive disbonding.

The program consisted of four series of tests. Each test series focused on different concerns and defect types. The first series was performed on a control panel which contained no known defects but which allowed LTI to establish the working parameters. Subsequent panel inspections included various defect types simulating actual aircraft fatigue cracks and disbonds. The sensitivity of the equipment to these defects was defined, as well as the general testing procedures for performing these tests.

The specific areas that the shearography demonstration program addressed included the following:

1. How shearography could be applied to an aircraft.
2. What stress would produce usable strain information.

3. What kinds of defects were detectable.

4. What the detection capability was for different defect types.

A further purpose of the program was to lay the ground work for the development of specific test methods and required equipment for these inspections.

TEST APPARATUS

Test Fixture

The test fixture was fabricated and operated by Foster-Miller, Inc. under separate contract from the VNTSC, as the FAA Aircraft Panel Test Facility (see figure 1). This fixture was designed to stress aircraft panels with the same hoop stresses an aircraft fuselage encounters as it goes to altitude and back.

The test fixture was a large weldment, which held the panel under test horizontally against a rubber seal that went around the edge of the panel. The panel was held in position (in plane) by turn buckles around all its edges (see figure 2). The fixture stressed the panel by pressurizing a reservoir of water beneath the panel which produced a hoop stress in the circumferential direction and a weak axial stress. Additional hydraulic cylinders were also used to increase the axial loading to more accurately simulate the pressurization tensional loading of an aircraft going to altitude. The hydraulic driver for this system was a computer controlled fatigue testing machine.

The fatigue tester provided good control during the test. For example, after setting a differential pressure and a rate of 0.1 hertz, the computer would cycle the same pressure differential every 10 seconds with good repeatability. Although the differential pressures used (0.005 to 0.060 psid) were nearly as low as the machine could control, they were typically below the accuracy of the system's pressure gauge.

Test Panels

The test panels inspected during this shearography demonstration were manufactured by East Coast Aero Tech and contained different defect types which represented specific aging aircraft problems. The two panels used during this shearography demonstration program simulated Boeing 727 and 737 fuselage construction (see figure 3). Each panel measured 6 x 10 feet and had a radius of curvature of 75 inches.

Panel No. 1 contained no programmed defects. This was used in Test Series No. 1 as a control, to define the inspection parameters for the demonstration program. This panel's construction was similar to that of a Boeing 727 fuselage. Prior to Test Series No. 2, Panel No. 1 had a single mid-bay crack placed in it as shown in figure 3. This crack, located in the mid-bay area of x2 to x3 in the axial direction, was dremel milled to 10 inches long and then fatigue sharpened. The fatigue sharpening was performed by pressurizing the panel approximately 200 times from 0 to 5 psig, simulating hundreds of flights

to 30,000 feet. The sharpened ends of the crack extended about 0.050 inches on both ends of the milled slot. Putty on the underside of the panel prevented the pressurized water from leaking past the crack.

Panel No. 2 was built to simulate a Boeing 737 fuselage section and contained mid-bay tear straps bonded to the skin between the frame members (see figures 4 and 5). This panel was built with a broad range of defects. These defects included:

1. Lap joint disbonding.
2. Multiple site damage (MSD), simulating fatigue cracking around top row lap joint rivets.
3. Lap joint cracking, simulating MSD linkup, where small cracks around rivets link together to form a large crack.

Panel disbonding was simulated by leaving adhesive off of areas of the lap joint and a tear strap during the panel's construction. This resulted in a programmed lap joint disbond length of approximately 30 inches. The small simulated MSD cracks were electrical discharge machine (EDM) notches which measured approximately 0.062 inches from beneath both sides of each rivet head. These were added to 16 consecutive top row rivets, from tear strap no. 4 to tear strap no. 3. Note that because the notches were not sharpened, they provided lower stress concentrations at their tips than would be expected of real cracks tips. The lap joint crack extended from the last MSD rivet near tear strap no. 3 to frame member F3, along the top row of rivets. This crack was cut prior to fabrication of the panel.

Each of these panels was held in the Foster-Miller test fixture and hydraulically stressed from its lower surface, while the shearography camera observed strain concentrations from the top surface.

Shearography Instrumentation

The inspection instrument used for the demonstration program was a portable LTI ES-9120 advanced shearography system as shown in figures 6 and 7.

Originally developed as a full field video strain gauge, the equipment measures micron level deformation of the material being inspected. This measurement of strain concentrations occurs in real-time over a large field of view, and is displayed to the operator on a video monitor.

The system utilizes a 200 mW Argon laser, fiber optic delivery system, shearography camera, and a shearography control unit (see figure 8). The camera utilizes a proprietary image shearing optical system to provide two overlapping and laterally displaced (sheared) images to a CCD camera, which records the resultant interferogram. Each point of the interferogram is created by having light from two different points on the object, overlaid by the optical shearing, added together. Since coherent (same color and phase) laser light is being used, the phase relationship of the two light waves is being compared. As the object under test deforms from an applied stress, the

intensity of the combined light from the two points being considered changes as the phase relationship between the two points changes.

The CCD camera is being used as a phase sensitive camera, which is able to detect $1/2$ wavelength of light changes at the surface of the object. Since the Argon laser light has a wavelength of 514 nm, surface strains of approximately a $1/4$ micron are detectable. The system's image processor records these changes for every point in the field of view and displays a real-time map of differential strain across the image. Each fringe represents one wavelength of light change or approximately 1 microstrain ($1/2$ micron/ $1/2$ inch), in the vector of the shearing. This shear (strain) vector can be rotated to measure the strain in any vector required. Typically either of two vectors are used, the X-vector, which measures the hoop strain and anomalies, or the Y-vector, which measures perpendicularly to the hoop strain (no hoop effect) and detects only the anomalies.

Real-time shearography is performed after the operator captures the first image to start an inspection. This records the initial strain state of the object. Each successive image, at video frame rates, is then compared with this initial stored image. As the object is stressed during the inspection, strain changes in the object are displayed as fringes defining the amount of plane strain that has developed since the initial reference image was captured. While watching the results on the video monitor, the operator can freeze the real-time shearogram at any time. This provides a double exposure shearogram that can be used to compare the final stored image with the initial stored image.

With an on screen video scaler, the operator can measure any anomalies in the field of view. Then, comparing the measured strain pattern with the live image of the object, the operator can locate any defects detected back onto the object. This not only helps to define the type of defect indicated, but allows the operator to mark the area for further analysis or repair. All the results are output as standard video signals, so they can be recorded in real-time on a VCR or video printer, as a permanent record of the inspection.



FIGURE 1. FAA AIRCRAFT PANEL TEST FACILITY AT FOSTER-MILLER

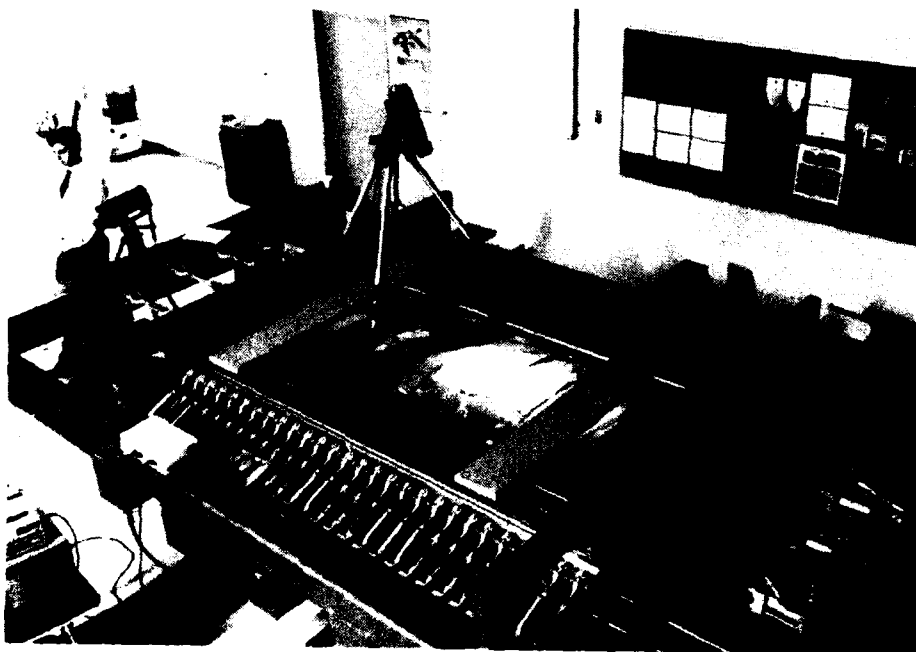


FIGURE 2. AERIAL VIEW OF TEST FIXTURE SHOWING TEST PANEL LAYING HORIZONTALLY WITH EDGES HELD AND THE ES-9120 ON THE FRAME.

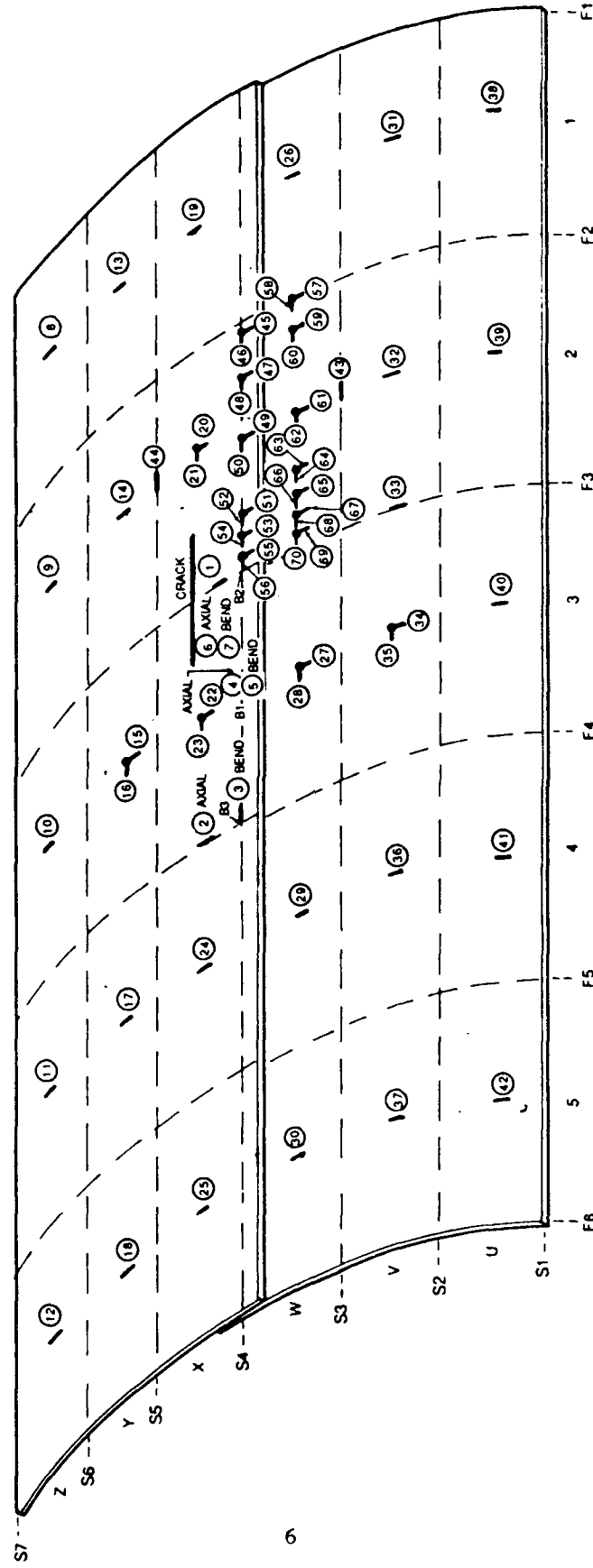


FIGURE 3. DRAWING OF TYPICAL TEST PANEL SHOWING LOCATIONS OF FRAMES (F1, F2, ETC.), TEAR STRAPS (1, 2, ETC.) AND STRINGERS (S1, S2, ETC.). CIRCLED NUMBERS CORRESPOND TO STRAIN GAUGE LOCATIONS USED DURING OTHER PANEL TESTING.

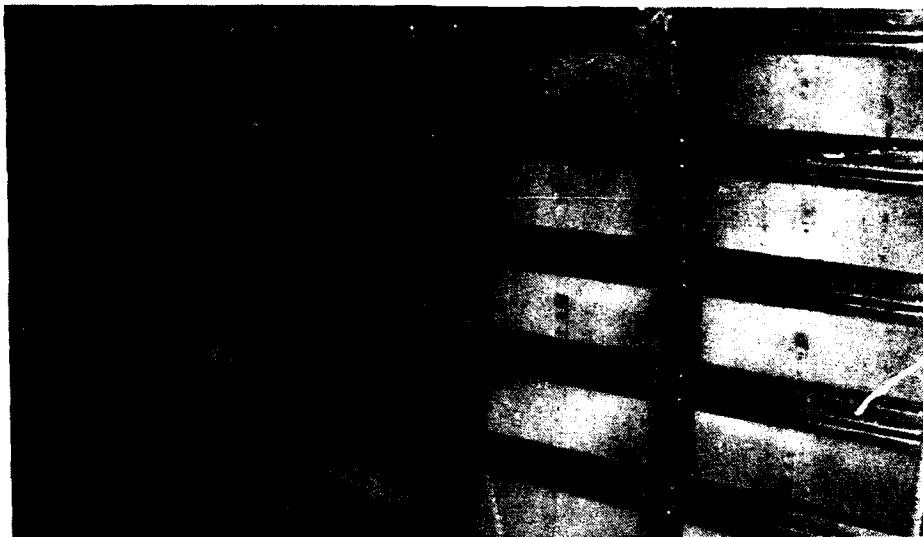


FIGURE 4. REAR VIEW OF TEST PANEL NO. 3. THIS PANEL IS SIMILAR IN CONSTRUCTION TO TEST PANEL NO. 2 AND WAS DESIGNED TO SIMULATE A BOEING 737. FRAME MEMBERS MOUNTED CIRCUMFERENTIALLY (VERTICALLY) AND STRINGERS MOUNTED AXIALLY (HORIZONTALLY) ARE SEEN IN THIS PHOTOGRAPH. TEAR STRAPS CAN ALSO BE SEEN PARALLEL TO THE FRAME MEMBERS AND BONDED TO THE SKIN.



FIGURE 5. CLOSE UP OF TEST PANEL CONSTRUCTION. THE LAP JOINT IS SHOWN BENEATH THE THIRD STRINGER FROM THE BOTTOM AND SHEAR CLIPS ATTACHING THE FRAME TO THE SKIN CAN BE SEEN BETWEEN THE STRINGERS.

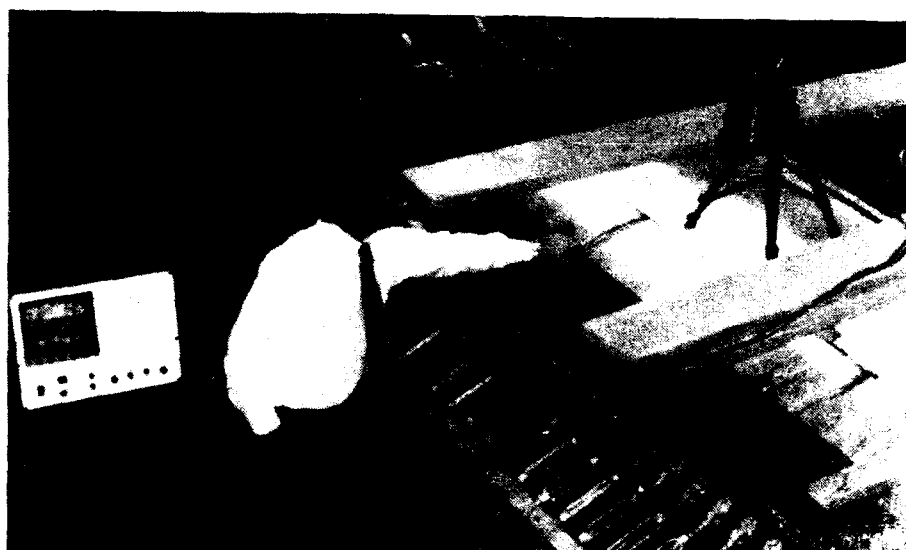


FIGURE 6. ES-9120 SHEAROGRAPHY SYSTEM INSPECTING FOR MSD CRACKING. NOT CONTROL UNIT ON CART WITH LASER BELOW.

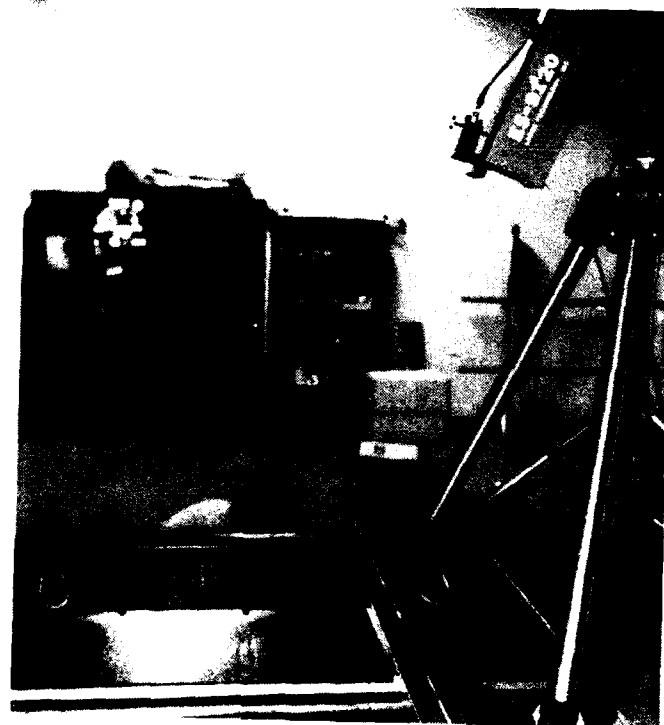


FIGURE 7. SHEAROGRAPHY CAMERA INSPECTING LAP JOINT. NOTE FIBER OPTIC DELIVERY SYSTEM MOUNTED ON TOP.

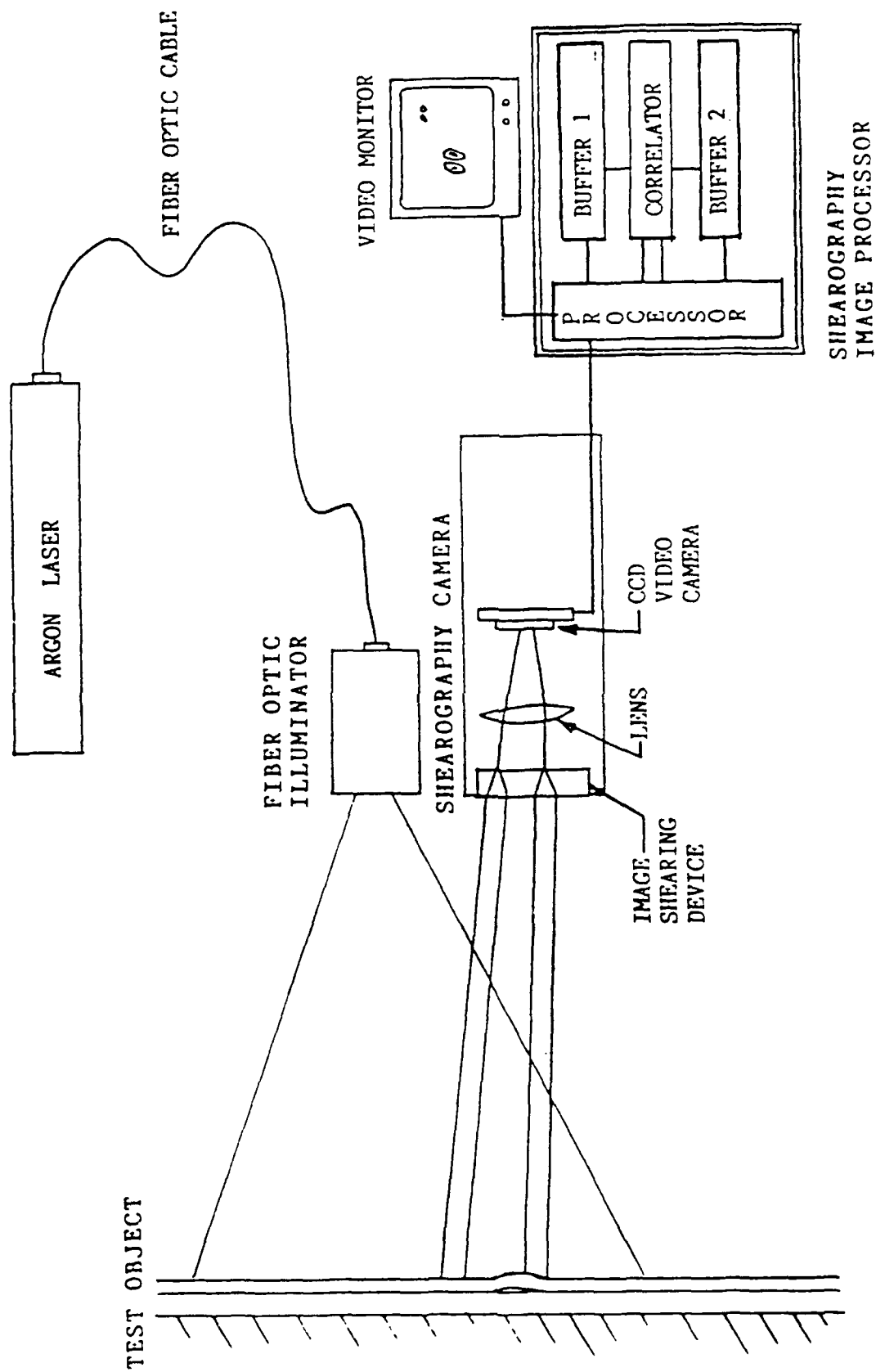


FIGURE 8. ILLUSTRATION OF SHEAROGRAPHY THEORY

TEST PROCEDURE

The primary test method used during these inspections was to place the tripod mounted shearography inspection head on the fixture or directly on the panel, to best view the area of interest.

The shearography control unit and the Argon laser were placed on a cart near the fixture. The camera's focus and iris were adjusted (see figure 9). The test fixture computer was set to provide the desired internal and differential pressures. Typically, the internal pressure was set nominally to 5 psig, while the desired differential pressure cycled at 0.1 hertz, varying over 10 seconds. This provided an even, repeating hoop stress which was perfect for analyzing the resultant strains. The differential pressure used was typically about 0.01 psid, which produced a small amount of strain across the lap joint of approximately 6 microstrains. This was far below the detection level of the surface mounted mechanical strain gauges which were placed on the first panel (see figure 10).

The areas inspected were coated with a soluble white spray (dye penetrant developer) to increase the reflectivity and diffusivity of the reflective aluminum surface. This coating provided presentation quality results, but would not be required for actual field inspections. Painted surfaces would also produce the same diffuse reflections as coated surfaces and are more easily inspected than bare aluminum structures.

For each inspection, the operator viewed the live image on the monitor, then switched to the shearographic image. He would store the initial strain state image at the lowest differential pressure. During the next ten seconds, as the differential pressure increased, the operator would view the strain increasing across the field of view in real-time. At the maximum differential pressure, the image is frozen, displaying a double exposure shearogram of the change in strain from the initial pressure to the final pressure.

Every inspection was videotaped for a complete record of each test series. Specific results were also photographed from the monitor for report documentation.

The operator would then pan the camera head to the next area of interest and repeat the inspection procedure above.



FIGURE 9. ADJUSTING SHEAROGRAPHY CAMERA ON THE TEST FIXTURE.

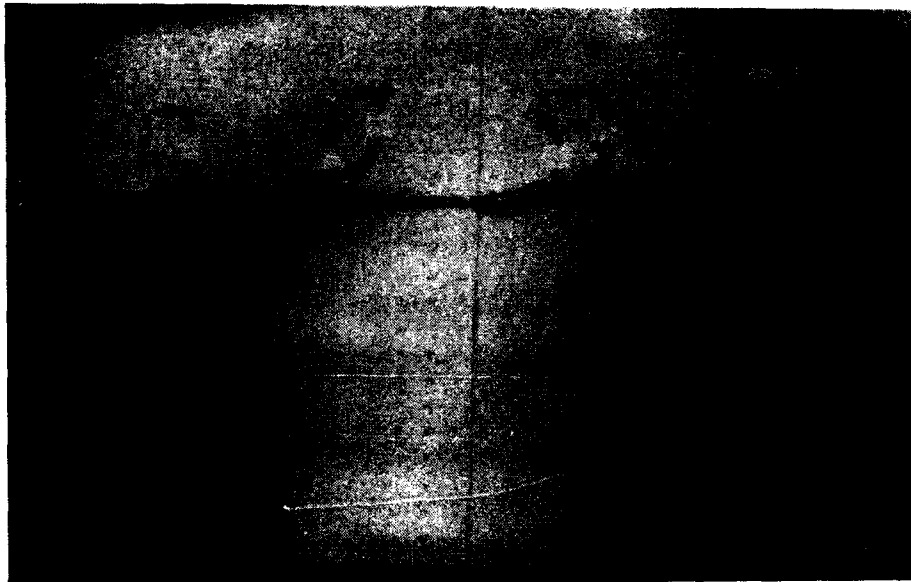


FIGURE 10. SHEAROGRAPHY CAMERA'S VIEW OF THE AIRCRAFT TEST PANEL WAS NOT AFFECTED BY THE PRESENCE OF STRAIN GAUGES WHICH WERE MOUNTED ON THE PANEL.

TEST SERIES NO. 1 - CONTROL PANEL

Results

The first test series was designed as a set of control inspections of a test panel with no known defects. The aircraft panel was mounted in the large Foster-Miller test fixture. The shearography camera and tripod were mounted on the fixture frame, where it was found to be quite stable. The camera was positioned to inspect different areas by aiming the tripod head at the area of interest. The typical field of view of the shearography camera for these inspections was 8 x 10 inches. The strain measurement by the shearography was unaffected by the surface mounted strain gauges and wires.

The test fixture, which allowed pressurizing of the panel hydraulically from underneath, was very precisely controllable. The internal pressure could be cycled from 0 to 8 psi, which simulated pressure differentials experienced by an aircraft going to altitude. For these shearographic inspections, the pressure was set to approximately 5 psig and the controller varied the pressure by approximately 0.01 psi at 0.1 hertz (10 seconds per cycle). This pressure variation was well below the strain gauges' sensitivity, but provided good stress levels for the shearography camera.

The first area of interest was the lap joint. The lap joint inspections were performed with both X-vector shearing, measuring variations in Z-axis deformation between 2 points separated in the X-axis or hoop direction (see figure 11), and Y-vector or axial direction shearing (see figure 12).

X-vector shearing showed evenly spaced vertical fringe lines, revealing the strain resulting from the applied hoop stress across the field of view. Y-vector shearing showed no fringes over an even strain field, since the shearing was aligned with the hoop strain. Strain concentrations from internal structures such as shear clips, which connect the skin to frame members, are visible in these figures. Defects would be revealed as variations in the strain fields.

The first area on the lap joint to be inspected showed an uneven strain concentration around a top row rivet. This strain concentration can be seen in figure 11 as a bowing of otherwise straight fringe lines in the X-vector shearogram. In the Y-vector shearogram, the strain concentration around the same rivet shows the characteristic double set of fringes as seen in figure 12. This strain concentration can be caused by a weakness in the strength of the rivet to hold the skins together. The rivet in question was later found to have been replaced during panel fabrication. The imaged strain around this rivet could have been caused by a loose fit, disbonding between the panels, or some other weakness.

Using the on screen video scaler, the location of the strain concentration was correlated from the live image (figure 13, top) to the X-vector shearogram (figure 13, middle) to the Y-vector shearogram (figure 13, bottom). In the live image, note that the lap joint is oriented vertically in the image, and that the strain gauges are located on either side of the image. In the X-vector image, note that the strain gauges do not interfere with the

inspection, although the wires are visible in areas. In correlating the images together, it is seen that the strain concentration is centered around a top row rivet, which ties the top skin to the edge of the underlying skin.

Other areas of the test panel were inspected, producing similar results, without finding any further questionable areas. The area in which a mid-bay crack would later be induced was inspected (figure 14 and 15) to provide base line data for the future analysis of the crack strain data. These shearograms were taken of mid-bay area x3, between frame members F3 and F4, and between stringers S4 and S5 with 0.06 psid.

Discussion

Test Series No. 1 proved very successful at defining the basic parameters for performing shearography on the fabricated aircraft test panel. First, the test method of stressing the panels internally worked well for both X-vector and Y-vector shearing, as well as mounting the shearography camera on the fixture frame away from the test panel. Second, a standard test pressure to produce even strain patterns for a variety of areas on the control panel was defined. Thirdly, resolution proved to be more than adequate to image internal structures as well as a potential weak area around a single rivet. This same strain resolution proved to be at least two magnitudes more sensitive than the surface mounted strain gauges.

Questions generated from Test Series No. 1 included the following: First, what is the sensitivity of advanced shearography to cracks, to disbonds, and to other structural weaknesses? Second, does shearography produce the same results at different internal pressures? Third, how large a field of view can be attained while maintaining acceptable resolution?

This initial work on aircraft test panels, as well as previous experiences on actual aircraft with electronic shearography, indicated that this inspection method is potentially a fast and comprehensive inspection for aircraft fuselage structures. These tests had already demonstrated that aging aircraft inspections could be performed with differential pressures a magnitude below those required for strain gauges and acoustic emission methods. Finally, the resolution to image strain concentrations around a single rivet are potentially good enough to find cracks, disbonding, and other structural defects.



F4

FIGURE 11. X-VECTOR SHEAROGRAPH OF AIRCRAFT PANEL LAP JOINT. LAP JOINT IS ORIENTED VERTICALLY, WITH HORIZONTAL IMAGE SHEARING. NOTE THE WEAK AREA AROUND THE TOP AND TEAR STRAPS EITHER SIDE ON THE BOTTOM. DIFFERENTIAL TEST PRESSURE IS 0.03 PSI AND THE FIELD OF VIEW IS APPROXIMATELY 10 X 24 INCHES.



F4

FIGURE 12. Y-VECTOR SHEAROGRAPH OF AIRCRAFT PANEL LAP JOINT. LAP JOINT IS ORIENTED VERTICALLY, WITH VERTICAL IMAGE SHEARING. NOTE WEAK AREA AROUND RIVET AT TOP, INDICATED BY THE DOUBLE FRINGE SET AND TEAR STRAPS ON EITHER SIDE AT THE BOTTOM. DIFFERENTIAL TEST PRESSURE IS 0.03 PSI.

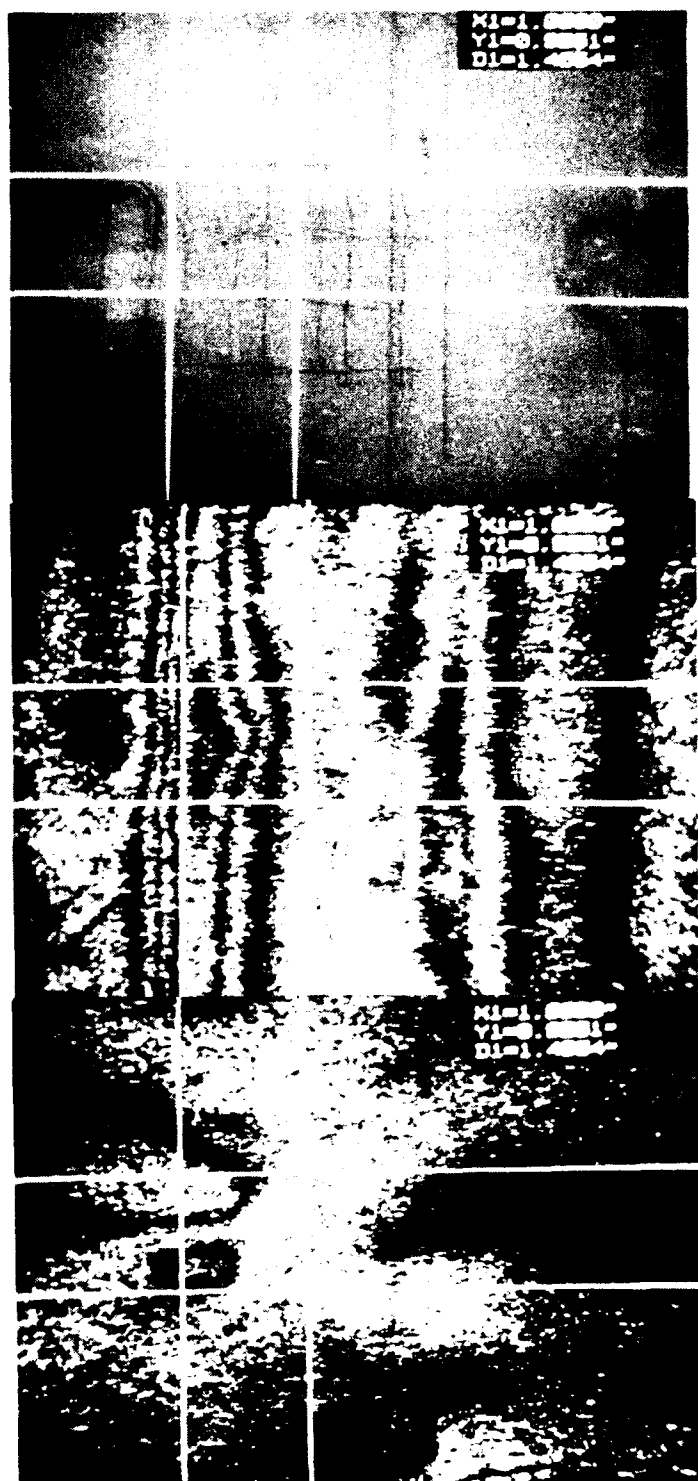


FIGURE 13. LIVE IMAGE (TOP), X-VECTOR SHEAROGRAPH (MIDDLE) AND Y-VECTOR SHEAROGRAPH (BOTTOM) OF THE SAME LOOSE RIVET IN TEST PANEL NO. 1.



FIGURE 14. X-VECTOR SHEAROGRAPH PRIOR TO WHERE A 10-INCH MID-BAY CRACK WOULD BE CUT INTO TEST PANEL NO. 1.

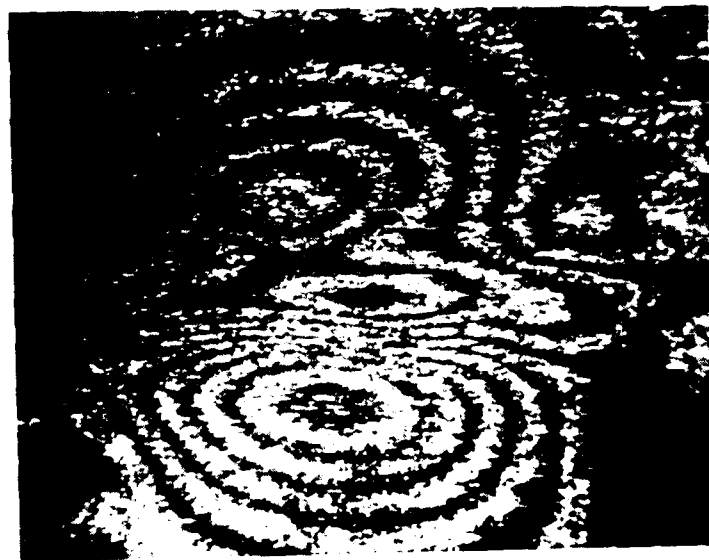


FIGURE 15. Y-VECTOR SHEAROGRAPH PRIOR TO WHERE A 10-INCH MID-BAY CRACK WOULD BE CUT INTO TEST PANEL NO. 1.

TEST SERIES NO. 2 - MID-BAY CRACK

Results

Test Series No. 2 was designed to test the capability of the electronic shearography to detect a mid-bay crack. The shearography equipment was set up as in Test Series No. 1, with the camera mounted on the fixture frame and not in direct contact with the panel. Into the original control test panel of Test Series No. 1, a crack was placed in the mid-bay area between x2 and x3 in the axial direction as previously shown in figure 3. Foster-Miller personnel started the crack by cutting a 10-inch long slice in the panel centered around frame F3 with a dremel saw. The panel was then fatigue cycled to sharpen the crack at both ends. About 200 cycles from 0-5 psi were required to grow the crack to about 0.0625 inches on each side. Putty on the underside of the panel prevented the pressurized water from coming through the crack, although some water leaked out around the tear strap attachment point (see figure 16).

The shearography inspections of Test Series No. 2 focused around this 10-inch mid-bay crack area shown in figure 17. The parameters being investigated were varied individually to determine their effect on the crack detection capability of the equipment. These parameters included varying the internal pressure, the differential test pressure, and the camera's shearing vector. These inspections were all performed from the same position on the panel fixture by tilting the shearography camera on the tripod, and with the fiber optic illuminator illuminating the camera's field of view. The panel was initially stressed to 5 psig and the differential stressing pressure varied approximately by 0.01 psi. This cyclic differential pressure loading of 0.01 psi at 0.1 hertz (10 seconds) was at the lower limit of the fixture's pressure measurement capability, and was a third of the differential loading pressure used during Test Series No. 1. Consequently, the strain indications of the internal structural components previously shown in figures 14 and 15 were substantially reduced. The crack, however, showed considerable deformation due to the hoop stress pulling the crack apart even with this minimal amount of loading (figure 18).

The crack was inspected with X-vector shearing initially at 0.01 psid stress level as described above. The indicated strain was more than was required for detection, so the inspected differential pressure was reduced to 0.005 psid (see figure 19), while shearing in the X-vector. This reduced the number of fringes in half producing a stress level that was one-sixth that of the first test series. Even the high strain internal structures such as the tear straps were barely visible.

The inspections continued with 45-degree vector shearing as shown in figure 20 and with Y-vector shearing as shown in figure 21. Note that the number of strain concentration fringe pairs in the shearographic images increased from two in X-vector shearing (figure 21) to three in the 45-degree vector of figure 20 and the Y-vector shearing shown in figure 21. This effect showed the crack opening up from the hoop stress, coupled with the tear strap in the center trying to hold the crack together. The shearographic images can all be related to the live image of the crack area shown previously in figure 17, although the shearography images of the strain patterns cover nearly twice the

area. Note that in the live image, the tear strap rivets are on either side of the crack in the center.

In order to determine what the effect would be of different internal pressures on the strain patterns seen by shearography, inspections were run at various internal pressures with the same differential stress pressure of 0.01 psi. Most inspections conducted in Test Series No. 1 had been run using 5 to 8 psig of internal pressure. It was desired to confirm that similar results could be achieved at lower pressures. During this set of inspections, the pressure was reduced from 5 psig to 4 psig, then to 3 psig, and finally to 1 psig of internal pressure. At each level, the same patterns were repeated, each duplicating the same resolution and crack sensitivity. A pressure of 0.6 psig was considered ambient due to the weight of the water.

The crack tip itself was also inspected optically. At 20X (figure 22) the crack tip looked very small, measuring about 0.05 inches long. At 200X (figure 23) and 0 psig internal pressure, the crack was nearly invisible, while at 5 psig as shown in figure 24, it opened dramatically.

Discussion

Test Series No. 2 continued defining the capabilities of advanced shearography. The mid-bay crack that was placed in the control panel produced substantial strain from a small amount of applied hoop stress. The shearography equipment proved effective at detecting this crack strain at various shearing vectors and at the full range of internal pressures, from 1 to 8 psig.

Imaging strain concentrations due to cracks is one focus of this research program at using advanced shearography to detect cracks quickly and effectively. As seen in the 200X micrographs, a crack can be nearly invisible at ambient pressure, even at high magnification. Advanced shearography will potentially be able to detect small cracks by their resultant strain concentrations from an applied hoop stress from either internal pressurizing of the aircraft, or from local external loading of the area of interest. This inspection could also cover a wide field of view, as much as 2 x 3 feet at one time.

Some of the questions generated from Test Series No. 1 have been answered, such as the detectability of larger cracks and shearography's effectiveness at various internal pressure conditions. Questions still to be resolved concerned shearography's sensitivity to detect smaller cracks including MSD, and its sensitivity to discern disbonds between riveted panels.

Test Series 2 demonstrated that electronic shearography can detect strain concentrations around cracks. Also, it can detect strain concentrations around individual rivets while maintaining a relatively large field of view. These tests have been performed with very small changes of applied hoop stress, and could be implemented on actual aircraft using various different stressing methods.

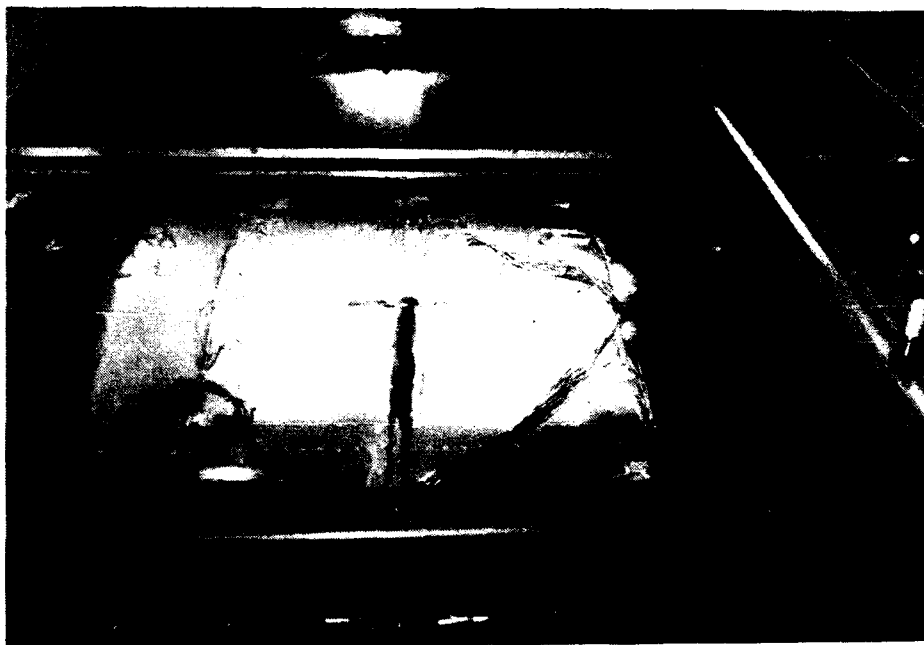


FIGURE 16. PHOTOGRAPH OF TEST PANEL NO. 1 WITH 10-INCH MID-BAY CRACK SHOWN HORIZONTALLY IN THE CENTER.



FIGURE 17. NORMAL VIEW OF THE MID-BAY CRACK AFTER FATIGUE CYCLING TO 15 INCHES. NOTE SEALING PUTTY SEEPING THROUGH ON BOTH SIDES OF THE TEAR STRAP ATTACHMENT POINT. WATER IS SEEN LEAKING FROM BENEATH THE TEAR STRAP. FIELD OF VIEW IS APPROXIMATELY 13 x 18 INCHES.



FIGURE 18. HIGH STRAIN SEEN OVER MID-BAY CRACK WITH 0.01 PSI DIFFERENTIAL STRESSING PRESSURE IN THIS X-VECTOR SHEAROGRAPH. FIELD OF VIEW IS 18 x 26 INCHES.



FIGURE 19. X-VECTOR SHEAROGRAPH of MID-BAY CRACK AT 0.005 PSI DIFFERENTIAL STRESSING PRESSURE. THE CRACK IS ORIENTED HORIZONTALLY WITH THE CRACK TIPS SHOWING AS SHARP POINTS BETWEEN EACH VERTICAL FRINGE PAIR. FIELD OF VIEW IS APPROXIMATELY 20 x 30 INCHES.

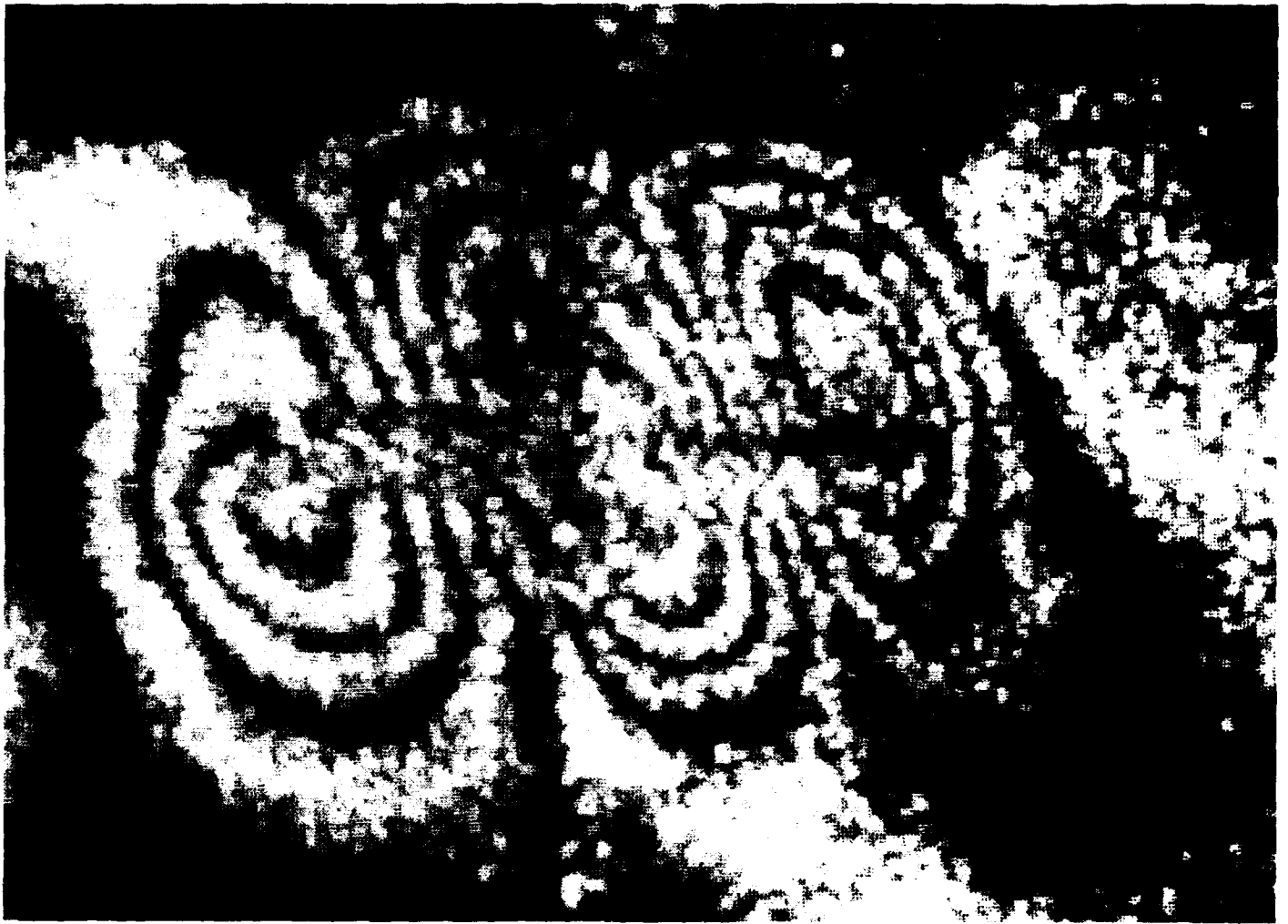


FIGURE 20. IMAGE OF A 45-DEGREE VECTOR SHEAROGRAPH SHOWING STRAIN CONCENTRATIONS AROUND THE MID-BAY CRACK. THIS IMAGE WAS TAKEN AT A 0.005 PSI DIFFERENTIAL STRESSING PRESSURE WITH A FIELD OF VIEW OF 13 x 19 INCHES.



FIGURE 21. Y-VECTOR SHEAROGRAPH AT 0.005 PSI DIFFERENTIAL PRESSURE, SHOWING STRAIN CONCENTRATIONS AROUND THE MID-BAY CRACK. THE DOUBLE SETS OF FRINGE PAIRS INDICATE THAT THE TEAR STRAP IS TRYING TO HOLD THE CRACK TOGETHER. FIELD OF VIEW IS APPROXIMATELY 16 x 24 INCHES.



FIGURE 22. 20X MICROGRAPH SHOWING CRACK TIP AREA. FIELD OF VIEW IS APPROXIMATELY 0.500 x 0.375 INCHES, WITH CRACK TIP MEASURING 0.050 INCHES.



FIGURE 23. 200X MICROGRAPH AT 0 PSIG SHOWING THE CRACK TIP CLOSED.



FIGURE 24. 200X MICROGRAPH AT 5 PSIG WITH THE CRACK TIP OPENED. FIELD OF VIEW IS APPROXIMATELY 0.050 x 0.065 INCHES.

TEST SERIES NO. 3 - SIMULATED LAP JOINT DISBONDS

Results

Test Series No. 3 was designed to test the capability of shearography to detect the presence of lap joint disbonds. The shearography camera was set up on the fixture as in previous tests, viewing an area of approximately 11 x 14 inches. Panel No. 2, simulating a 737 fuselage section, was constructed leaving an area of the lap joint without adhesive to simulate adhesive disbonding. The panel was built with other defect types, but these did not interfere with the disbond inspection, except for the MSD linkup at the end of the test. The fixture pressure was typically held at a nominal 5 psig, in order to stay consistent with the other tests.

Test Series No. 3 focused on the 30-inch section of the lap joint that was unbonded. To provide an accurate comparison, an adjacent section of the lap joint that was properly bonded was also inspected. The inspection proceeded rapidly, documenting a 4 foot section of the lap joint in about 30 minutes. The differential pressure that was used for this test series was 0.04 psi.

The results from Test Series No. 3 are shown in composite image shearograms that extend onto two pages (figures 25 and 26). The composite image appears confusing at first, so black markings have been drawn on the images to ease interpretation.

The images contain quite a bit of detail about the internal structure. A good image to start with is the Y-vector image of figure 25. The images are 14 inches across, with the lap joint running up the center. Note the transition line is drawn as a black vertical line on the right hand side of the lap joint. This is due to the edge of the upper skin section. The large structural elements, seen as double lobed fringe sets vertically displaced on either side of the lap joint, are due to tear strap no. 5 at the bottom and the shear clips attached to frame F5 in the middle. These will typically look the same throughout the panel, unless there is a defect associated with the structure; also, note these same structures in the X-vector shearogram shown in figure 25. The dark area in the fringes of the right shear clip (better seen in the X-vector shearogram) is water leaking from an unsealed area of the lap joint near the shear clip.

The lower left fringe set of the upper tear strap no. 5 does not look as if it is evenly loaded, possibly indicating a defect in its construction. This was not a programmed flaw and its exact origin is currently unknown. Looking at more detail in the Y-vector shearogram of figure 25, notice that the top half of the lap joint area has many small radius fringes, and that the bottom half does not. The top half corresponds to the programmed disbond area, while the bottom half was well bonded. The unbonded upper skin around the rivets is lifting up from the 0.04 psid load. Some disbonded areas showed greater strains than others did as depicted in the right side of the lap joint at the top of the Y-vector shearogram. This area, which covers two rivets, indicates substantial deformation, possibly coupled with weak rivets. Another area showed residual strain, which developed after a few cycles of loading, and was centered over a single rivet (see figure 27).

An important, potentially more reliable interpretation method for the detection of disbonds can be seen in the X-vector shearograms of both figures 25 and 26. Disbonding allows the upper skin to move in relation to the lower skin, and hence, generate inter-skin fringe lines seen between the images of the upper skin edge. These areas are highlighted in black as two vertical lines in the left of figure 25. As seen in that figure, these inter-skin fringes only form next to the disbonded areas.

In figure 26, the entire length of the lap joint is disbonded. Again, the composite shearogram is 14 inches wide, with the lap joint running up the center. In the Y-vector image, note the extensive fringing around the rivets (small circular fringes), which indicate the presence of local disbonds. The larger structures, from the bottom, are the tear strap no. 4, which appears to be evenly loaded, and shear clips attached to frame F4 in the middle. Also inter-skin fringes, indicative of disbonding, run the entire length of the X-vector shearogram in figure 26.

At the top of the Y-vector image, note the extensive fringes extending onto the lap joint. This was an area of simulated MSD linkup, which was a milled slot through multiple top row rivets. This indication was very obvious, showing as easily as the mid-bay crack in Test Series No. 2. At this pressure, there were too many fringes to clearly resolve, so it was not investigated further.

Discussion

Test Series No. 3 demonstrated the capability of shearography to readily detect lap joint disbonding. This was seen over a large area of the lap joint with good resolution. The series also demonstrated the speed of the inspection method, covering 11 x 14 inch areas in less than a minute each, while manually providing both X and Y-vector shearograms. Finally, the observation of the excessive amounts of strain from the MSD linkup area, completed the demonstration of shearography's ability as a wide field inspection tool.

Shearography has demonstrated its ability to quickly detect larger structural defects from weak rivets, cracks, and disbonded areas.

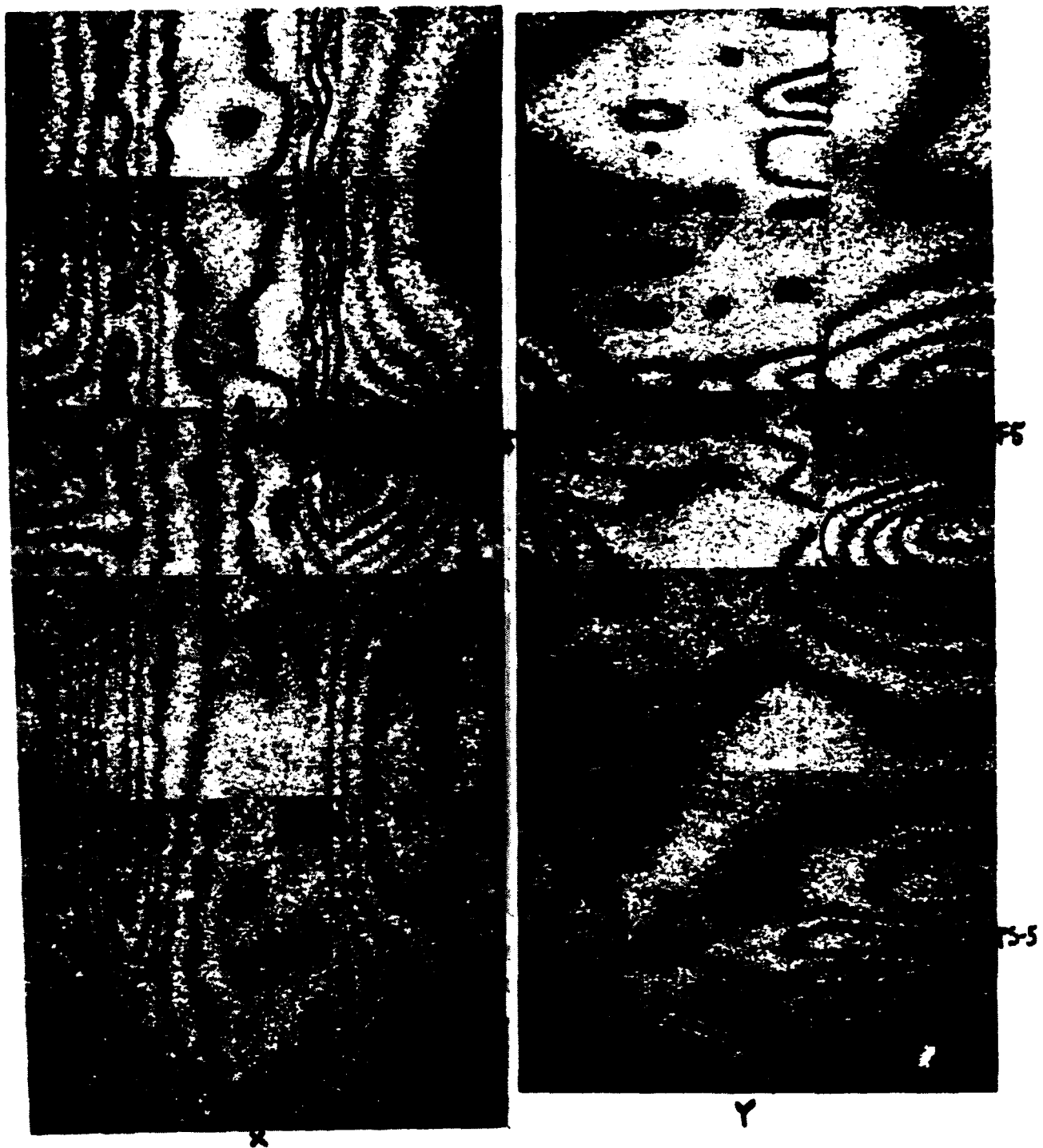


FIGURE 25. FIRST SECTION OF LAP JOINT INSPECTED DURING TEST SERIES NO. 3 SHOWING BONDED AND DISBONDED AREAS. LEFT SIDE IMAGE IS OF THE X-VECTOR SHEAROGRAPH AND THE RIGHT SIDE IMAGE SHOWS THE Y-VECTOR SHEAROGRAPH OF THE SAME SECTION.

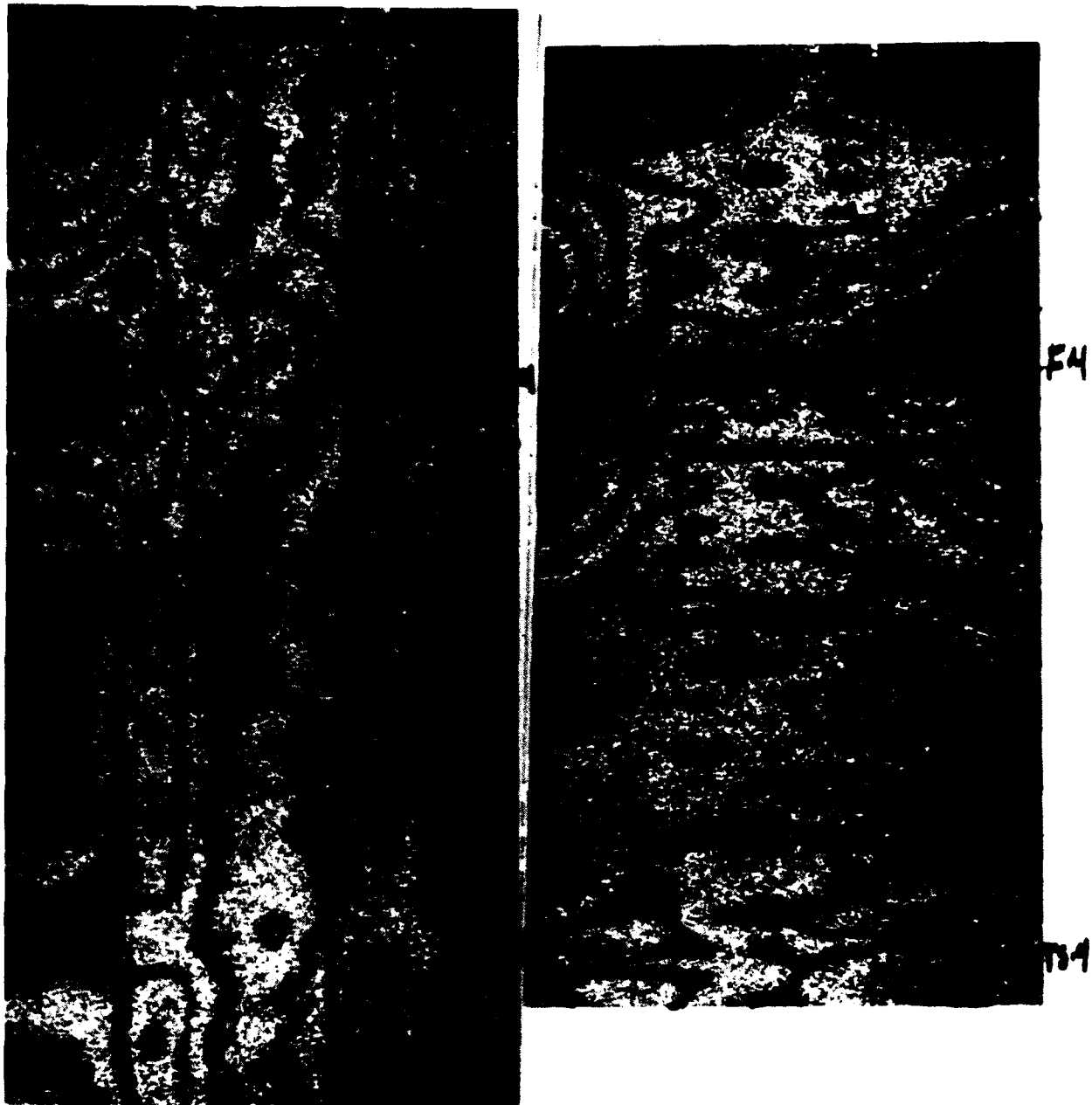


FIGURE 26. SECOND SECTION OF LAP JOINT INSPECTED DURING TEST SERIES NO. 3 SHOWING DISBONDING AND MSD LINKUP AT THE TOP OF EACH IMAGE. LEFT SIDE IMAGE IS OF X-VECTOR SHEAROGRAPH AND THE RIGHT SIDE IMAGE IS OF THE Y-VECTOR SHEAROGRAPH.

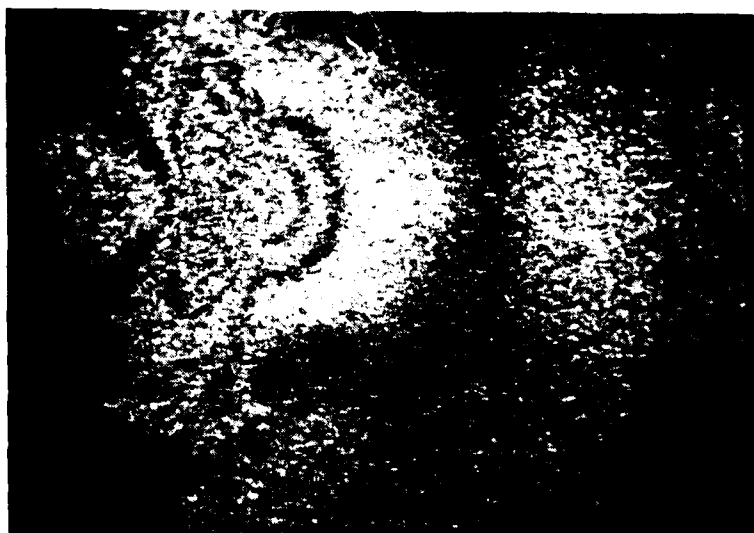


FIGURE 27. RESIDUAL STRAIN INDICATING A LAP JOINT DISBOND AROUND A SINGLE RIVET OR POSSIBLY AN IMPROPERLY LOADED RIVET.

TEST SERIES NO. 4 - SIMULATED LAP JOINT MSD

Results

The fourth test series was designed to test the capability of shearography to detect small cracks around rivets. These tests were preceded by lab work on panels with some small fatigue sharpened cracks which are shown in figures 28 and 29. These results, using both thermal and tensional loading, showed the strain concentrations of 0.375-inch long cracks. Initial lab tests indicated that the camera would have to be moved closer than during previous tests in order to resolve these smaller strain concentrations.

Panel No. 2 was constructed with 0.0625-inch EDM notches cut into the sides of a number of top row rivets, parallel with the lap joint or axial direction. These simulated unsharpened EDM notches provided minimum strain patterns and offered a worse case scenario for crack detection by shearography.

The setup for Test Series No. 4 changed from the previous tests, in that the shearography camera was mounted on a smaller tripod and placed directly on top of the test panel (see figure 30). This provided a closer look in order to view the small strain concentrations around the EDM notches. It also reduced the field of view to only six rivets. The nominal internal pressure was maintained at 5 psig, and the differential pressure was maintained at 0.04 psid.

The results were phase changes over the notches on either side of the rivets as shown in figure 31. These phase changes or shifts in the grey tone of the image, represent a fraction of one fringe or a fraction of one microstrain across the crack.

Discussion

The MSD notches were difficult to detect, although larger sharpened cracks were more easily detected. Continued work will be done in this area to increase the detectability of these small MSD cracks. Other stressing mechanisms such as heat and vacuum were not possible to implement on this test fixture due to the presence of the large water mass on the underside of the panel. These and other stressing mechanisms, such as induction heating, may be able to increase the strain concentration at the MSD cracks to improve the sensitivity of the inspection beyond the pressurization stressing of this test. Also, it is believed that the detection of actual sharpened fatigue cracks may be easier than the unsharpened EDM notches that were used to simulate them.

Each inspection can potentially be quick. It seems that shearography, with typical stressing techniques, will be capable of small area inspection for the detection of small MSD cracks.

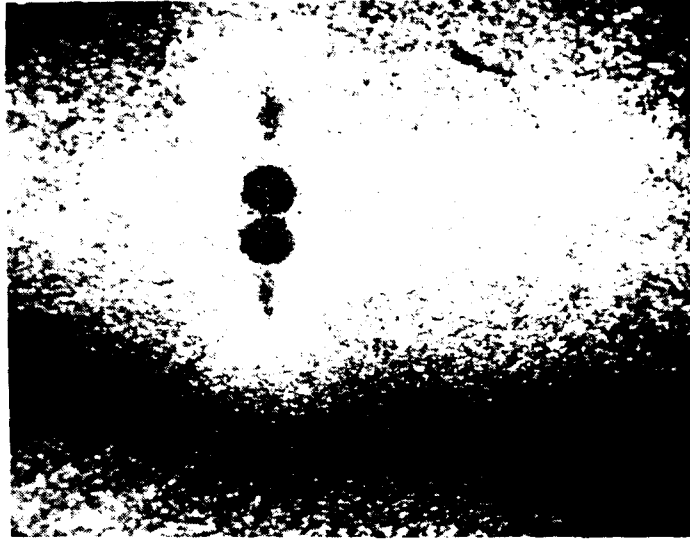


FIGURE 28. SMALL FATIGUE CRACKS AROUND PANEL RIVET HOLE. Y-VECTOR SHEAROGRAPH WITH CRACK MEASURING ABOUT 0.375 INCHES.

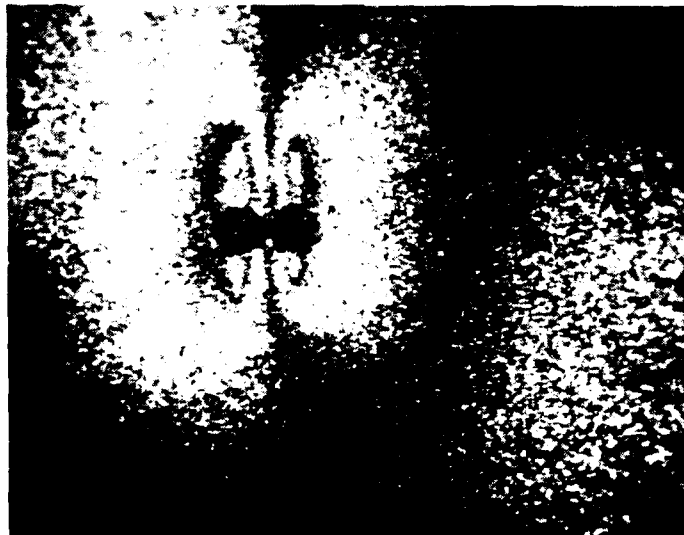


FIGURE 29. X-VECTOR SHEAROGRAPH SHOWING STRAIN CONCENTRATIONS AROUND 0.375-INCH CRACKS.

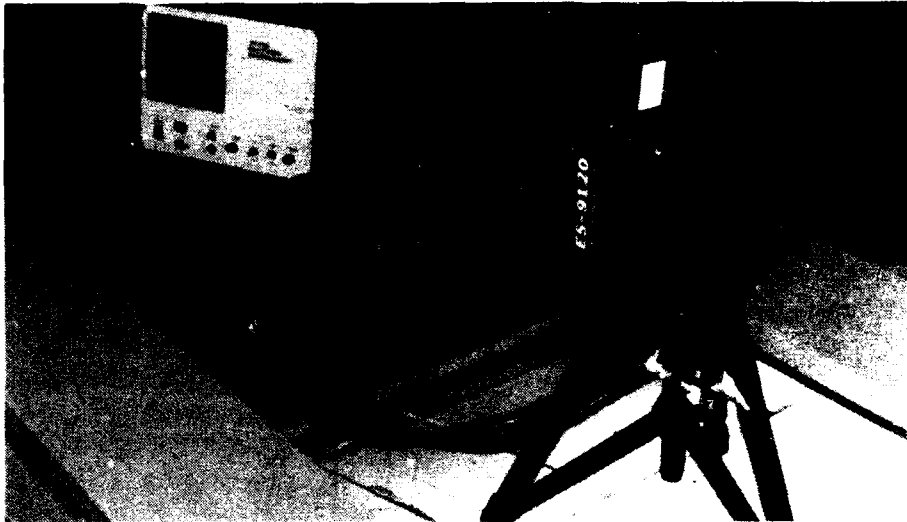


FIGURE 30. SHEAROGRAPHY CAMERA SITTING ON PANEL TO CLOSELY VIEW MSD CRACKING.



FIGURE 31. SMALL MSD CRACKING ALONG UPPER LINE OF RIVETS (CENTER AND RIGHT). CRACKS WERE SIMULATED WITH EDM NOTCHES BUT WERE NOT FATIGUE SHARPENED.

CONCLUSIONS

This shearography demonstration program provided LTI with simulated defects in aircraft fuselage panels and a controllable test fixture to internally stress the structure. This realistic setup allowed LTI to properly develop shearographic inspection techniques to detect the various types of fatigue and disbonding defects plaguing aging aircraft. These tests have provided a valuable baseline of data upon which future work will be based.

The results of this program have demonstrated first that electronic shearography is applicable to the wide field inspection of aircraft fuselage structures for the detection of fatigue related defects. And second, that the speed of this optical inspection technique proved to be unhampered during its application at the FAA's Aircraft Panel Test Facility.

Lap joint disbonds were readily located using shearography during these tests. Disbonding caused the lap joint rivets to take all of the load across the lap joint which generated strain concentrations around the rivets and between the overlapped skins.

Improperly loaded rivets were detected showing excessive strain across them. These rivets were not carrying the applied load as well as the rest of the rivets. Sound rivets showed no strain changes across them, indicating a continuous load bearing structure.

Mid-bay cracks were easily detected by the shearography system. These weaknesses caused excessive differential strain extending well beyond the crack tip itself, and were detected with very low stress levels.

Cracks linking multiple rivets in the lap joint, coupled with unbonding, showed high strain concentration, acting similarly to the mid-bay crack described above. The strain concentrations extended across the lap joint and well into the mid-bay area.

Small simulated MSD cracks were detected with close inspection of the shearography system. When loaded, the strain concentrations around these unsharpened EDM notches were small. This reduced the typically wide field view of the shearography system and allowed inspection of just 6 rivets at a time.